Fingerprints of Majorana modes beyond the zero-bias conductance peak

Satoshi Ikegaya

Max Planck Institute for Solid State Research

Max-Planck-Institut für Festkörperforschung

SPICE SPIN PHENOMENA INTERDISCIPLINARY CENTER

Oxide Superspin Core-to-Core Programme JSPS-EPSRC

Collaborators

- **Dirk Manske** (MPI)
- **Yasuhiro Asano** (Hokkaido Univ.)
- **Yukio Tanaka** (Nogoya Univ.)
- **Shun Tamura** (Nogoya Univ.)

Contents

Sec. 0

Motivation

Topological superconductors

(e.g. chiral p-wave)

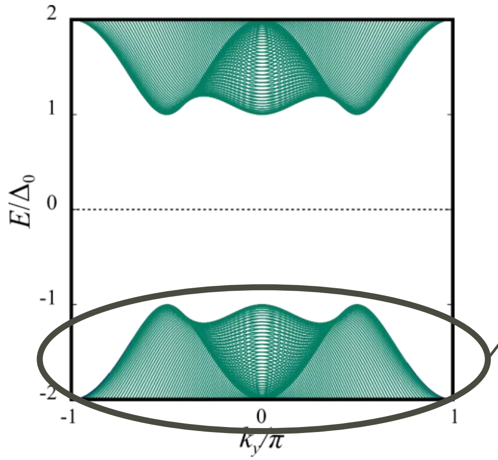

Topological number

$$\mathbb{Z} \neq 0$$

Nontrivial
"bulk" band topology

Topological superconductors

(e.g. chiral p-wave)

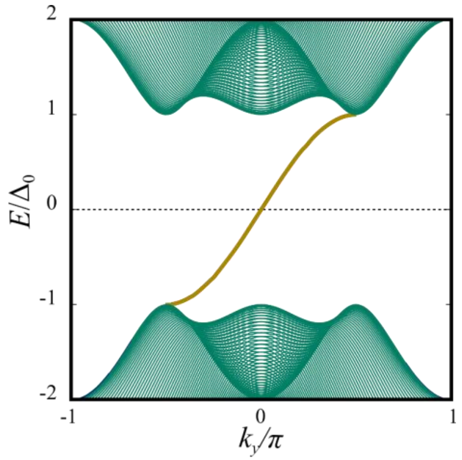

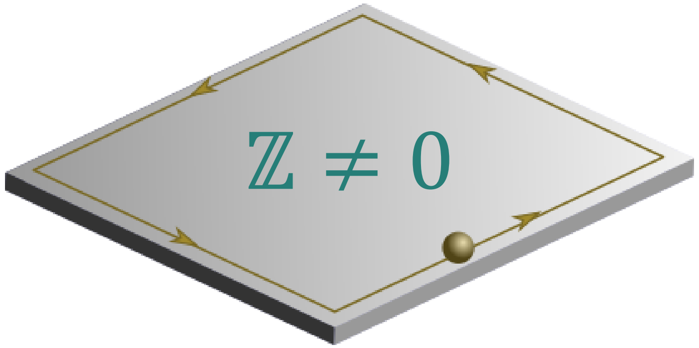

Nontrivial
"bulk" band topology

↔

Gapless
"boundary" states

Great attention due to:

- emergence of **Majorana bound states**($\gamma = \gamma^{\dagger}$),
- potential applications to **quantum computations**, etc.

Various edge states

Chiral p-wave	Helical p-wave	p_x-wave

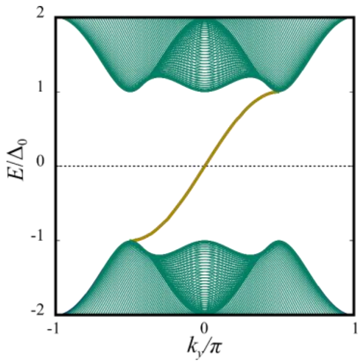

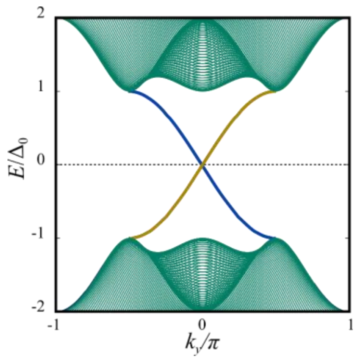

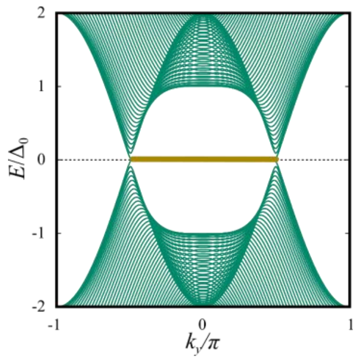

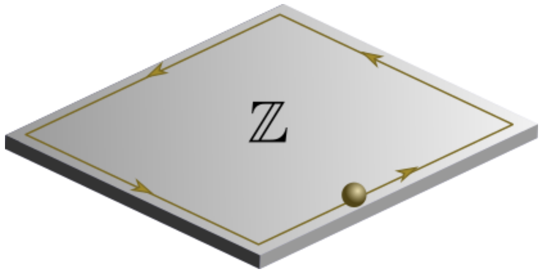

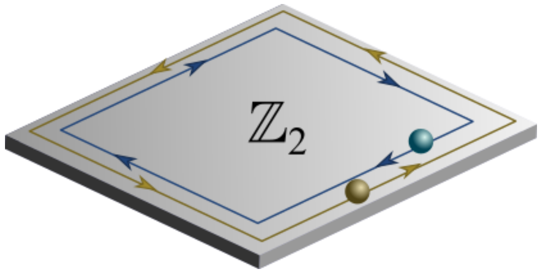

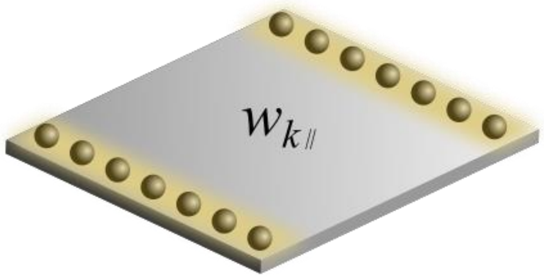

Chiral states

Helical states

Flat-band states
and more.

How can we detect them?

Tunneling spectroscopy

Conventional

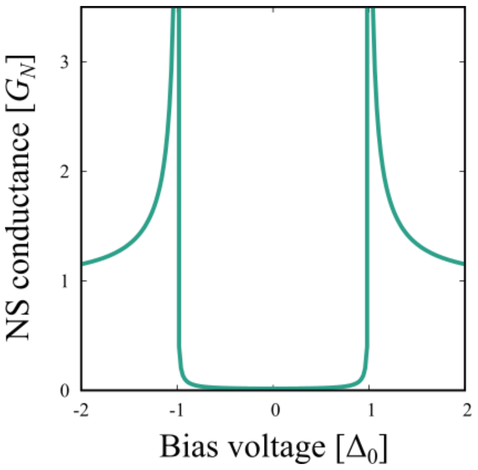

Gapped

Tunneling spectroscopy

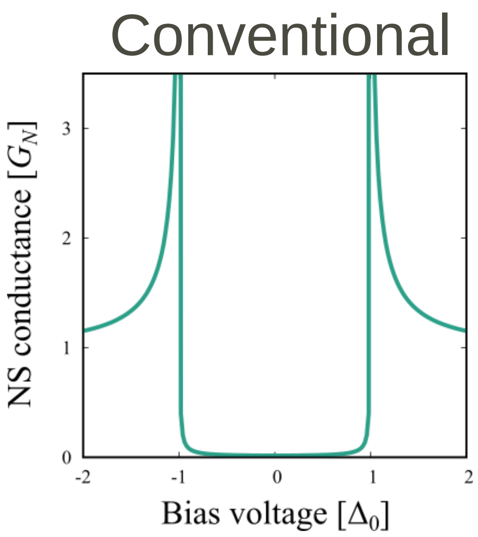

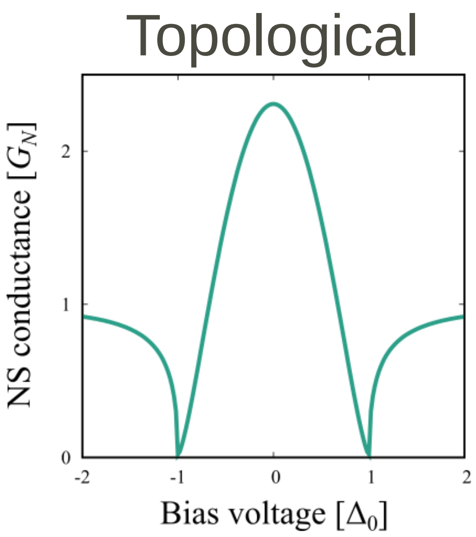

Gapped

Zero-bias peak

Powerful experiment! Actually…

Experimental observations so far

- Sr_2RuO_4 (Chiral)

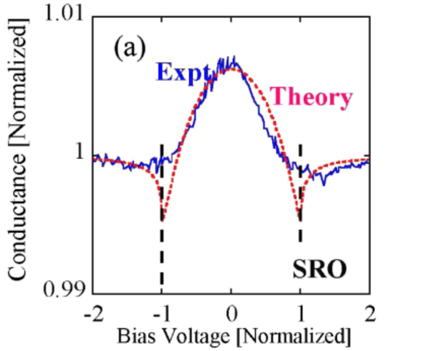

S. Kashiwaya, *et al*. PRL(2011)

- $Cu_xBi_2Se_3$ (Helical)

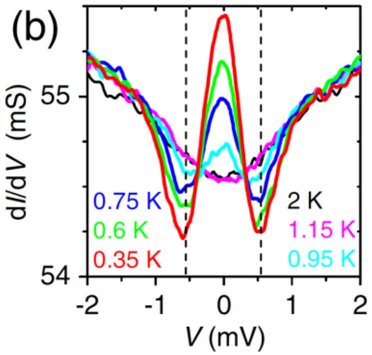

S. Sasaki, *et al*. PRL(2011)

- YBCO (Flat)

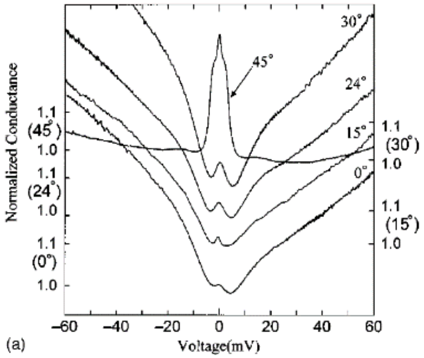

I. Iguchi, *et al*. PRB(2000)

- Semiconductor/SC hybrids

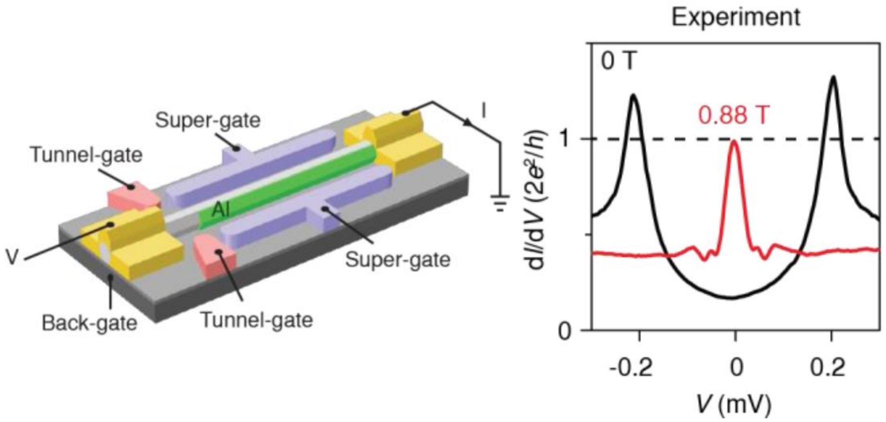

H. Zhang, *et al*. Nature(2018)

- Magnetic atoms/SC hybrids

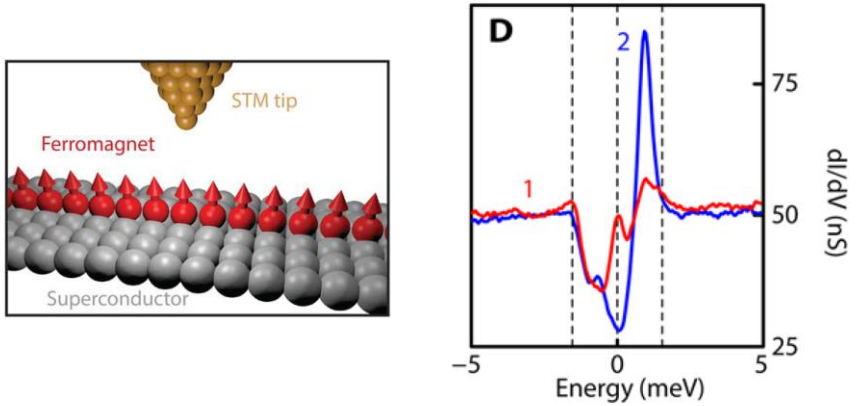

S. Nadj-Perge, *et al*. Science(2014)

and more.

Motivation

For the **past decade**,
the **existence** of topological edge states
has been **demonstrated** in various systems.

⬇

The time has come to **go beyond** proving their **existence**
and **embark on** investigating the **nature** of
topological edge states **more thoroughly**.

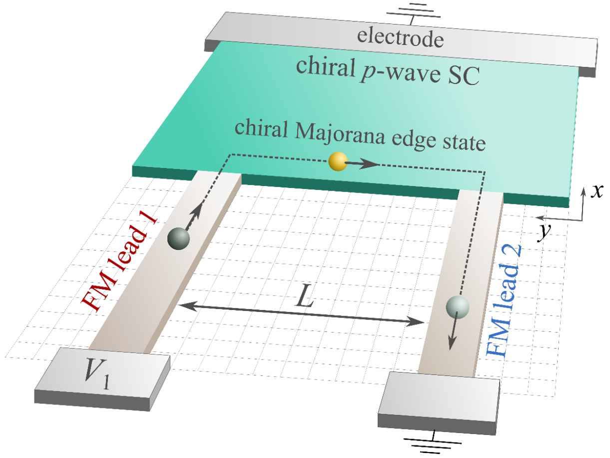

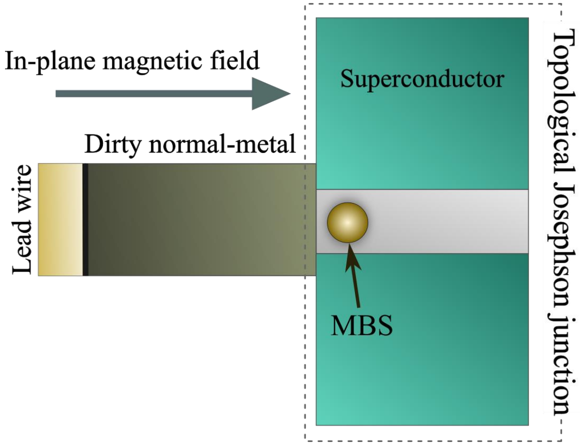

Sec. 1

Anomalous nonlocal conductance as a fingerprint of chiral Majorana edge states

S. Ikegaya, Y. Asano, and D. Manske

Phys. Rev. Lett. 123, 207002 (2019)

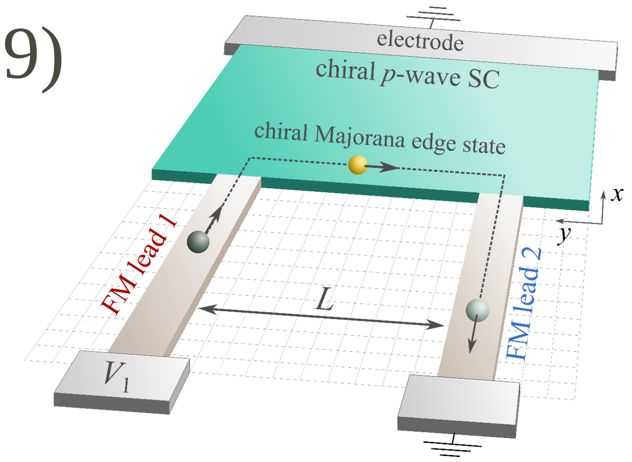

Objective (1)

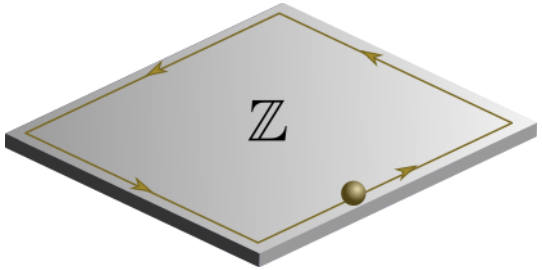

Chiral states

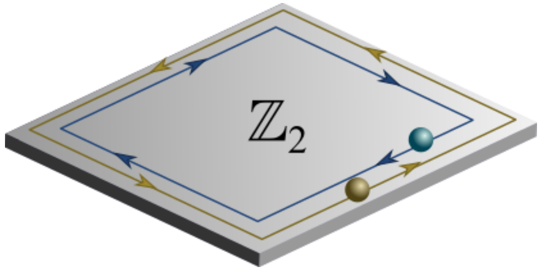

Helical states

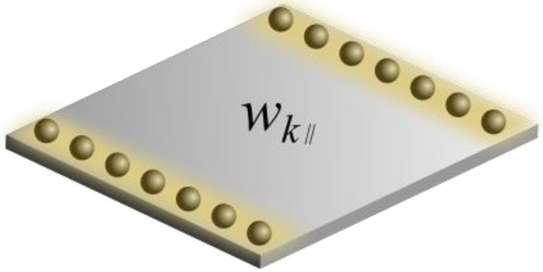

Flat-band states

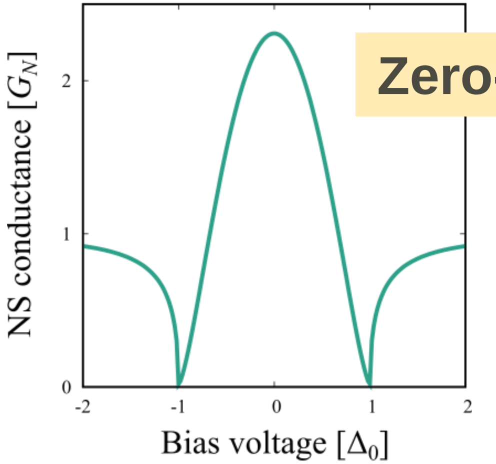

Zero-bias peak

Powerless to capture the "individuality" edge states.

Objective (1)

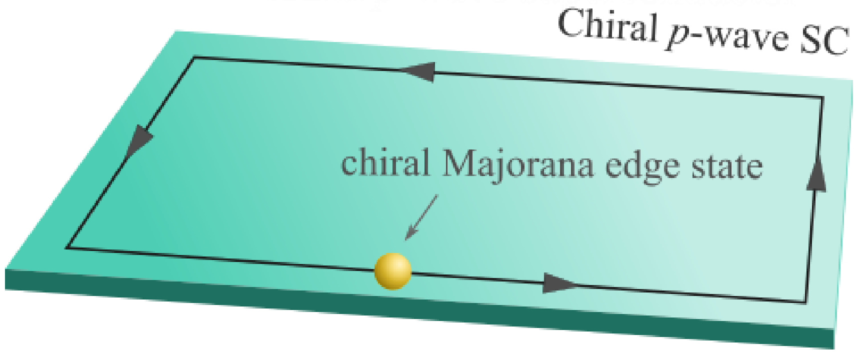

Proposing a “**smoking-gun**” experiment
for identifying “**chiral**” Majorana edge states

Idea

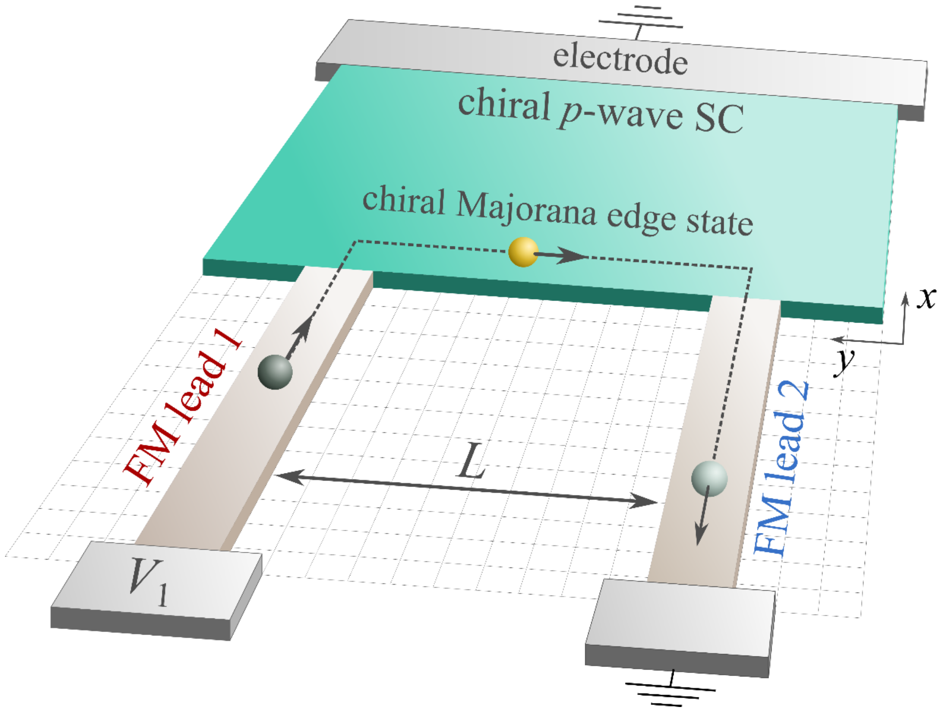

Nonlocal transport in a
ferromagnet/chiral p-wave superconductor hybrid

Model

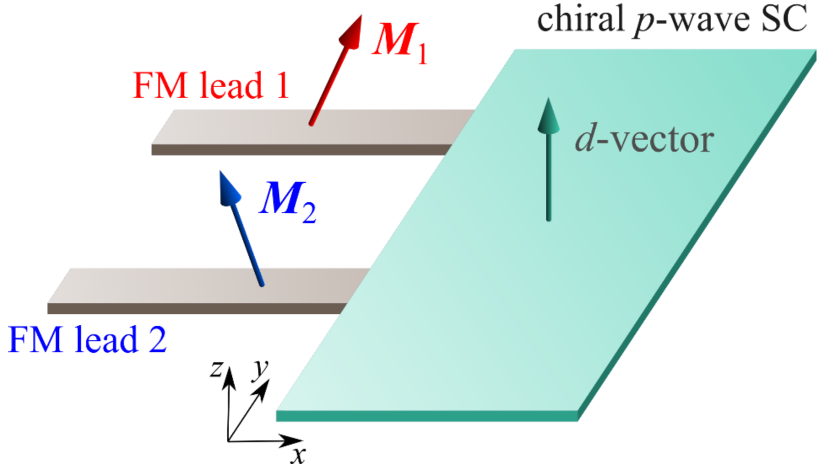

$$H_{\mathrm{FM}\alpha} = \sum_{\boldsymbol{k}} \sum_{\sigma,\sigma'} \left(\xi(\boldsymbol{k}) + \boldsymbol{M}_\alpha \cdot \hat{\boldsymbol{\sigma}}\right)_{\sigma,\sigma'} c^\dagger_{\boldsymbol{k}\sigma} c_{\boldsymbol{k}\sigma'}$$

$$H_{\mathrm{SC}} = \sum_{\boldsymbol{k},\sigma} \xi(\boldsymbol{k}) c^\dagger_{\boldsymbol{k}\sigma} c_{\boldsymbol{k}\sigma'} + \frac{1}{2} \sum_{\boldsymbol{k}} \sum_{\sigma,\sigma'} \left[\Delta_{\sigma\sigma'}(\boldsymbol{k})\, c^\dagger_{\boldsymbol{k}\sigma} c^\dagger_{-\boldsymbol{k}\sigma'} + \mathrm{h.c.}\right]$$

$$\Delta_{\sigma\sigma'}(\boldsymbol{k}) = \left\{\boldsymbol{d}_{\boldsymbol{k}} \cdot \hat{\boldsymbol{\sigma}}\, (i\hat{\sigma}_y)\right\}_{\sigma,\sigma'}$$

$$\boldsymbol{d}_{\boldsymbol{k}} = \Delta_0(\sin k_x + i\chi \sin k_y)\hat{\boldsymbol{z}}$$

Formulation: BTK formula

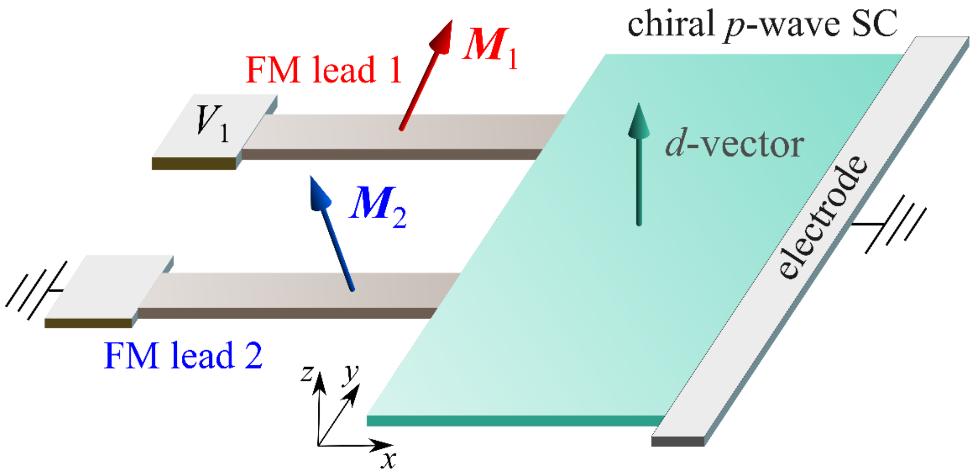

$$G_{\beta\alpha}(V_\alpha) = \frac{dI_\beta}{dV_\alpha}$$

I_β : current in lead β

V_α : applied bias voltage to lead α

(lead β and superconductor are grounded.)

Formulation: BTK formula

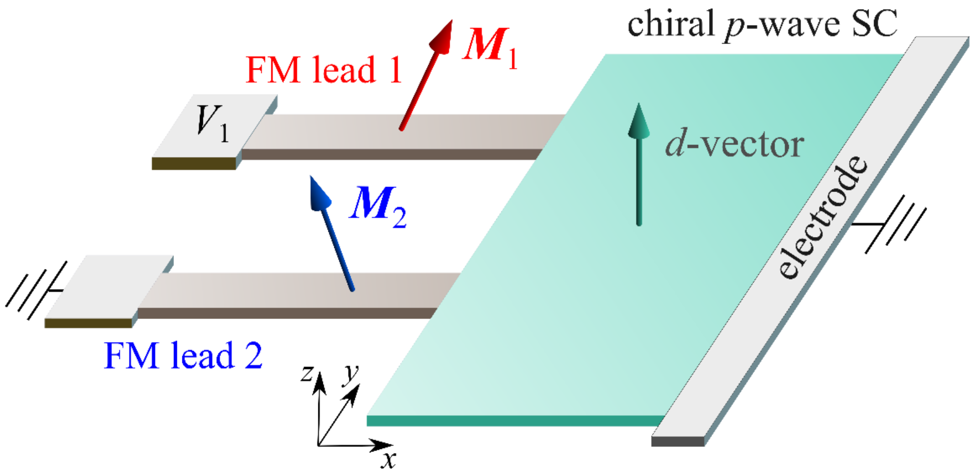

$$G_{\beta\alpha}(V_\alpha) = \frac{e^2}{h}\left[-R^{\mathrm{EC}}_{\beta\alpha} + R^{\mathrm{CAR}}_{\beta\alpha}\right]_{eV_\alpha = E}$$

G. Deutscher and D. Feinberg, App. Phys. Lett. **76**. 487 (2000)

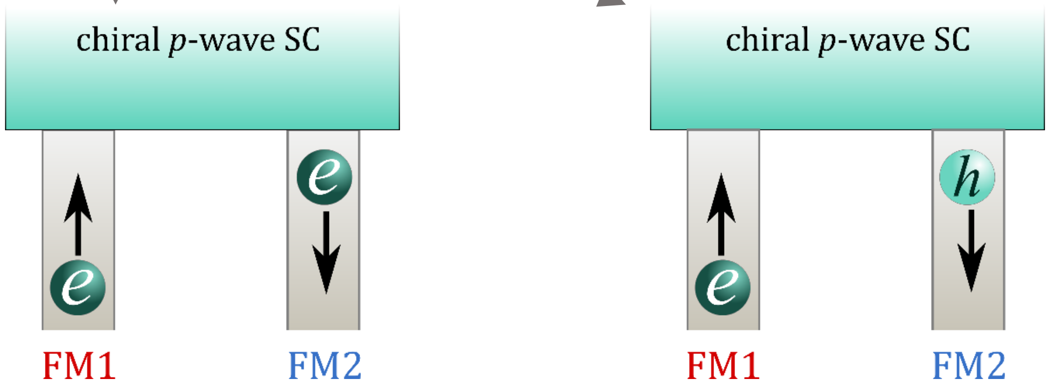

Expectation

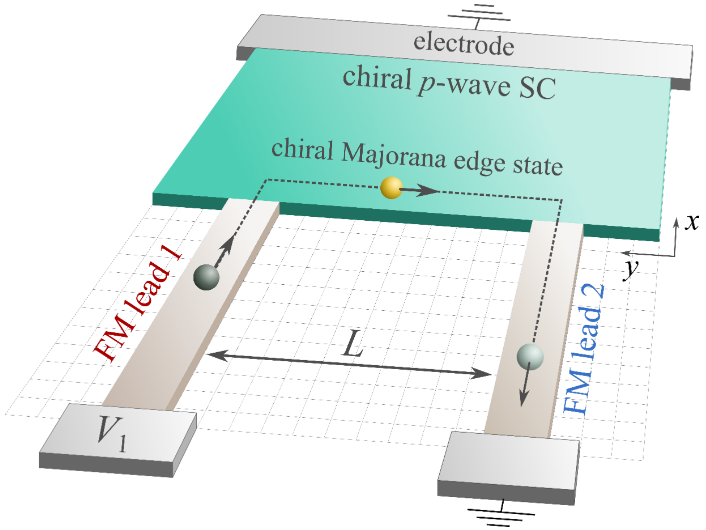

CMESs moving from the lead 1 to lead 2:

- **assist the nonlocal transport** from the lead 1 to lead 2.

  ➡ **G_{21} is finite irrespective of L.**

- **never assist the nonlocal transport** from the lead 2 to lead 1.

  ➡ **G_{12} is almost zero.**

Results

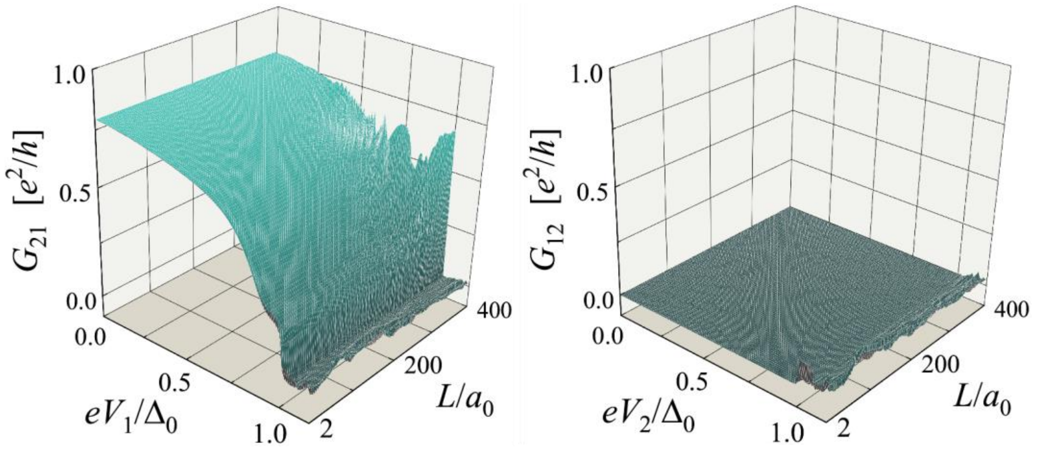

$\boldsymbol{M}_1 = -\boldsymbol{M}_2 = M_{\mathrm{ex}}\hat{\boldsymbol{z}}$,

$M_{\mathrm{ex}} = 0.5\mu$

$0.2\xi_0 \leq L \leq 40\xi_0$

CMESs moving from the lead 1 to lead 2:

- **assist the nonlocal transport** from the lead 1 to lead 2.

➡ $\boldsymbol{G_{21}}$ **is finite irrespective of $\boldsymbol{L}$.**

- **never assist the nonlocal transport** from the lead 2 to lead 1.

➡ $\boldsymbol{G_{12}}$ **is almost zero.**

Advantages of our proposal

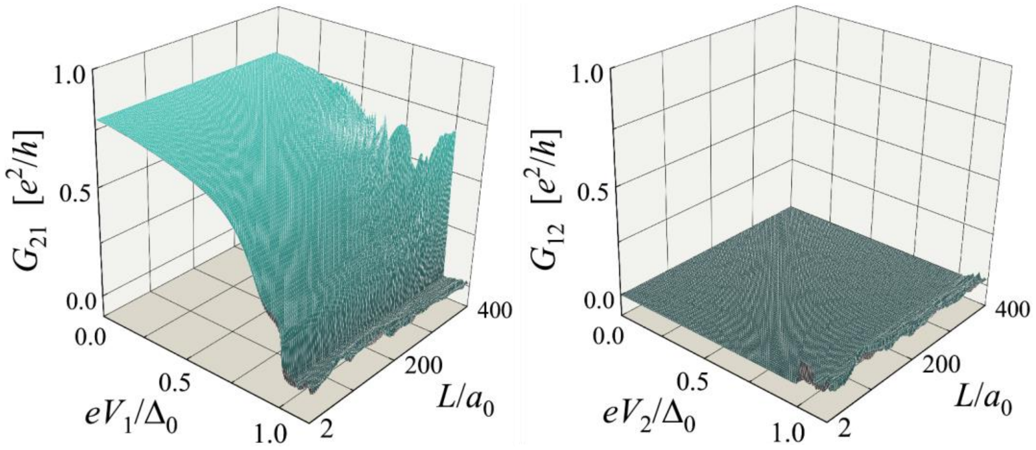

$\boldsymbol{M}_1 = -\boldsymbol{M}_2 = M_{\mathrm{ex}}\hat{\boldsymbol{z}}$,

$M_{\mathrm{ex}} = 0.5\mu$

$0.2\xi_0 \le L \le 40\xi_0$

(I) **Unique phenomenon** for chiral edge states

(II) We only need the **distinct contrast** in G_{21} and G_{12}.

Promising strategy for identifying CMESs

M_α dependence: Amplitude

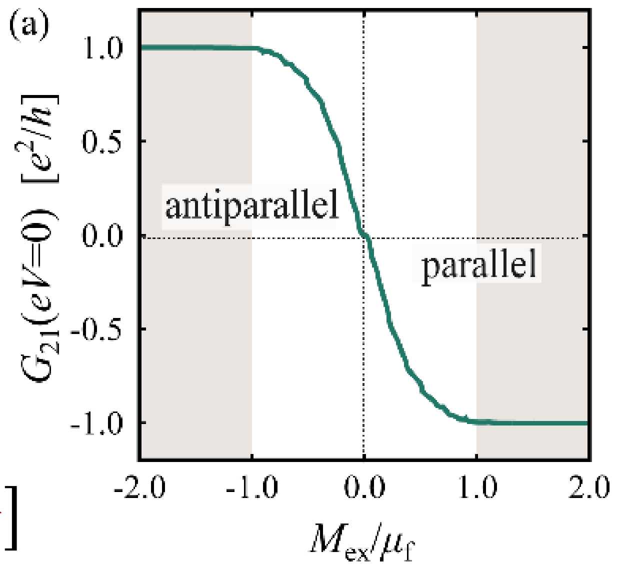

$\boldsymbol{M}_1 = |M_{ex}|\hat{\boldsymbol{z}},$

$\boldsymbol{M}_2 = M_{ex}\hat{\boldsymbol{z}}$

$$G_{21} = \frac{e^2}{h}\left[-R_{21}^{\mathrm{EC}} + R_{21}^{\mathrm{CAR}}\right]$$

half-metal	antiparallel	$M_{ex} = 0$	parallel	half-metal
$G_{21} = \frac{e^2}{h}$	$G_{21} > 0$	$G_{21} = 0$	$G_{21} < 0$	$G_{21} = -\frac{e^2}{h}$
$R^{\mathrm{EC}} = 0$ $R^{\mathrm{CAR}} = 1$	$R^{\mathrm{EC}} < R^{\mathrm{CAR}}$	$R^{\mathrm{EC}} = R^{\mathrm{CAR}}$	$R^{\mathrm{EC}} > R^{\mathrm{CAR}}$	$R^{\mathrm{EC}} = 1$ $R^{\mathrm{CAR}} = 0$

M_α dependence: Amplitude

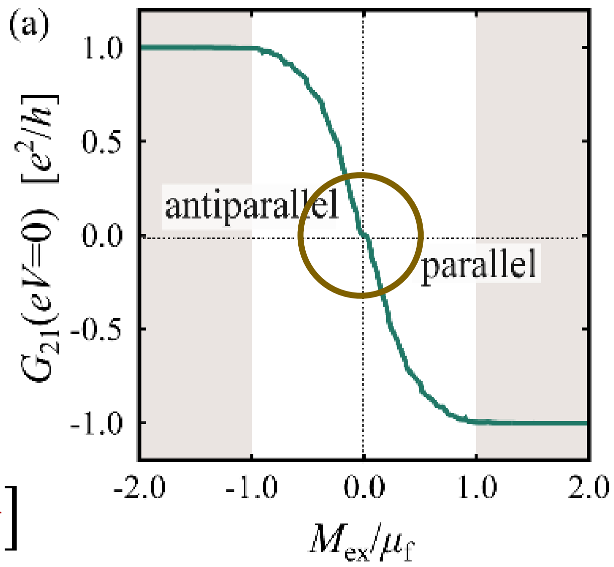

$\boldsymbol{M}_1 = |M_{ex}|\hat{\boldsymbol{z}},$

$\boldsymbol{M}_2 = M_{ex}\hat{\boldsymbol{z}}$

$$G_{21} = \frac{e^2}{h}\left[-R_{21}^{\mathrm{EC}} + R_{21}^{\mathrm{CAR}}\right]$$

half-metal	antiparallel	$M_{ex} = 0$	parallel	half-metal
$G_{21} = \frac{e^2}{h}$	$G_{21} > 0$	$G_{21} = 0$	$G_{21} < 0$	$G_{21} = -\frac{e^2}{h}$
$R^{\mathrm{EC}} = 0$ $R^{\mathrm{CAR}} = 1$	$R^{\mathrm{EC}} < R^{\mathrm{CAR}}$	$R^{\mathrm{EC}} = R^{\mathrm{CAR}}$	$R^{\mathrm{EC}} > R^{\mathrm{CAR}}$	$R^{\mathrm{EC}} = 1$ $R^{\mathrm{CAR}} = 0$

M_α dependence: Amplitude

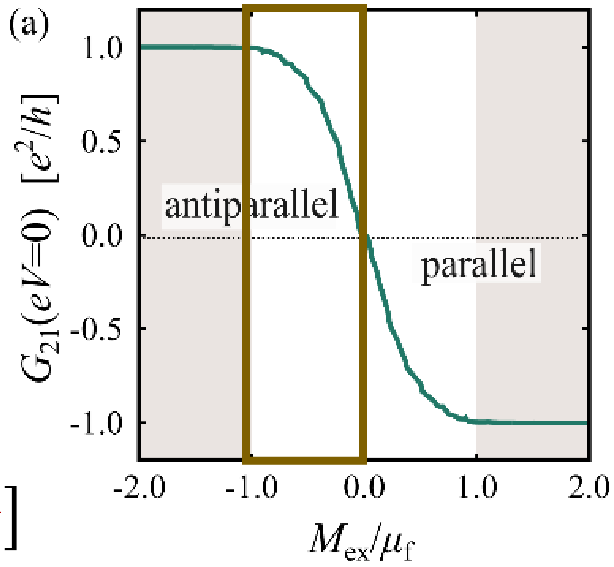

$\boldsymbol{M}_1 = |M_{ex}|\hat{\boldsymbol{z}}$,

$\boldsymbol{M}_2 = M_{ex}\hat{\boldsymbol{z}}$

$$G_{21} = \frac{e^2}{h}\left[-R_{21}^{\mathrm{EC}} + R_{21}^{\mathrm{CAR}}\right]$$

half-metal	antiparallel	$M_{ex} = 0$	parallel	half-metal
$G_{21} = \frac{e^2}{h}$	$G_{21} > 0$	$G_{21} = 0$	$G_{21} < 0$	$G_{21} = -\frac{e^2}{h}$
$R^{\mathrm{EC}} = 0$ $R^{\mathrm{CAR}} = 1$	$R^{\mathrm{EC}} < R^{\mathrm{CAR}}$	$R^{\mathrm{EC}} = R^{\mathrm{CAR}}$	$R^{\mathrm{EC}} > R^{\mathrm{CAR}}$	$R^{\mathrm{EC}} = 1$ $R^{\mathrm{CAR}} = 0$

M_α dependence: Amplitude

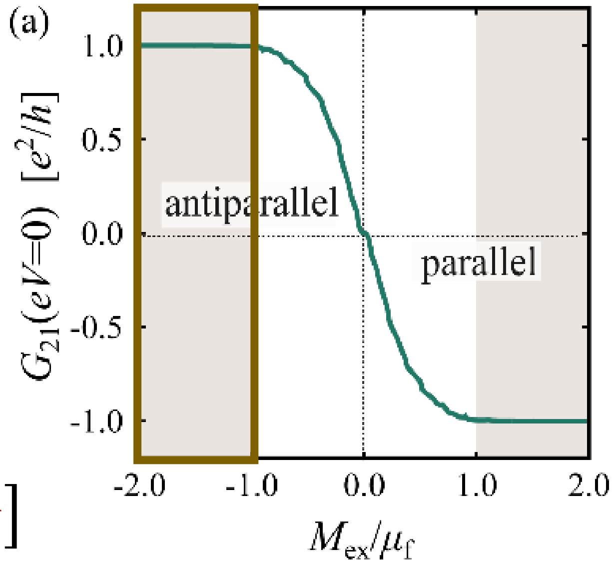

$\boldsymbol{M}_1 = |M_{ex}|\hat{\boldsymbol{z}},$

$\boldsymbol{M}_2 = M_{ex}\hat{\boldsymbol{z}}$

$$G_{21} = \frac{e^2}{h}\left[-R_{21}^{EC} + R_{21}^{CAR}\right]$$

half-metal	antiparallel	$M_{ex} = 0$	parallel	half-metal
$G_{21} = \frac{e^2}{h}$	$G_{21} > 0$	$G_{21} = 0$	$G_{21} < 0$	$G_{21} = -\frac{e^2}{h}$
$R^{EC} = 0$ $R^{CAR} = 1$	$R^{EC} < R^{CAR}$	$R^{EC} = R^{CAR}$	$R^{EC} > R^{CAR}$	$R^{EC} = 1$ $R^{CAR} = 0$

M_α dependence: Amplitude

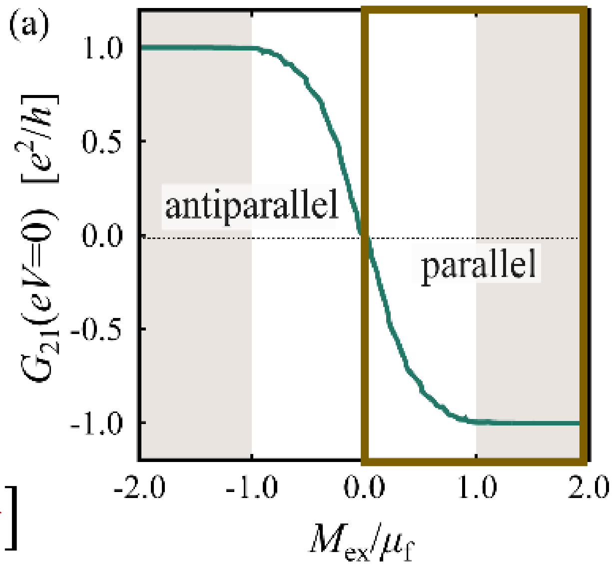

$\boldsymbol{M}_1 = |M_{\rm ex}|\hat{\boldsymbol{z}},$

$\boldsymbol{M}_2 = M_{\rm ex}\hat{\boldsymbol{z}}$

$$G_{21} = \frac{e^2}{h}\left[-R_{21}^{\rm EC} + R_{21}^{\rm CAR}\right]$$

half-metal	antiparallel	$M_{ex} = 0$	parallel	half-metal
$G_{21} = \frac{e^2}{h}$	$G_{21} > 0$	$G_{21} = 0$	$G_{21} < 0$	$G_{21} = -\frac{e^2}{h}$
$R^{\rm EC} = 0$ $R^{\rm CAR} = 1$	$R^{\rm EC} < R^{\rm CAR}$	$R^{\rm EC} = R^{\rm CAR}$	$R^{\rm EC} > R^{\rm CAR}$	$R^{\rm EC} = 1$ $R^{\rm CAR} = 0$

M_α dependence: Amplitude

When $d \parallel \pm M_\alpha$,

	EC process	CAR process	
	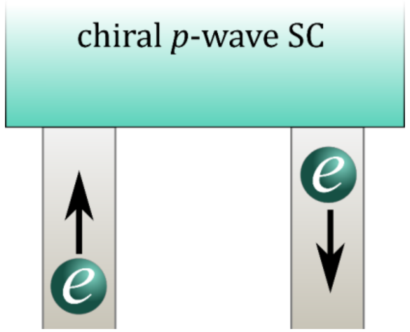	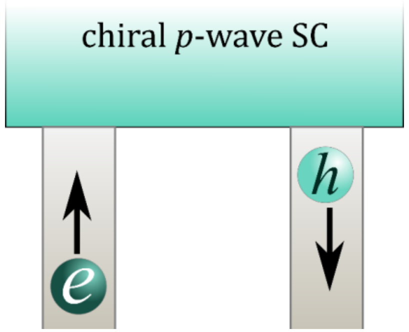	
	electrons have **same spin**	electron and hole have **opposite spin**	
Parallel			$R^{\mathrm{EC}} > R^{\mathrm{CAR}}$
Antiparallel			$R^{\mathrm{EC}} < R^{\mathrm{CAR}}$

M_α dependence: Direction

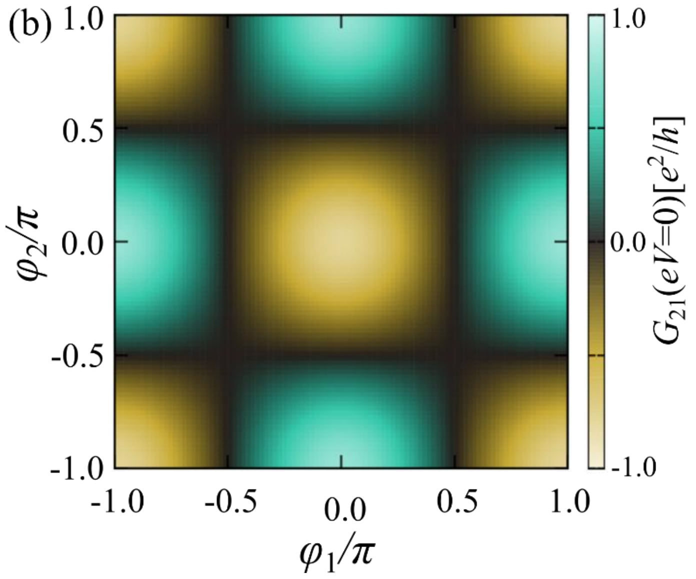

$$\boldsymbol{M}_1 = M_{\mathrm{ex}}(\sin\varphi_1, 0, \cos\varphi_1)$$

$$\boldsymbol{M}_2 = M_{\mathrm{ex}}(0, \sin\varphi_2, \cos\varphi_2)$$

- Maximum magnitude for $\boldsymbol{M}_1 \parallel \boldsymbol{d}$ and $\boldsymbol{M}_2 \parallel \boldsymbol{d}$
- Zero only for $\boldsymbol{M}_\alpha \perp \boldsymbol{d}$

Distinct contrast between G_{12} and G_{21} remains
for **the broad range of the magnetization alignments**.

Wave function

Wave function at zero energy having largest contribution to R^{CAR}

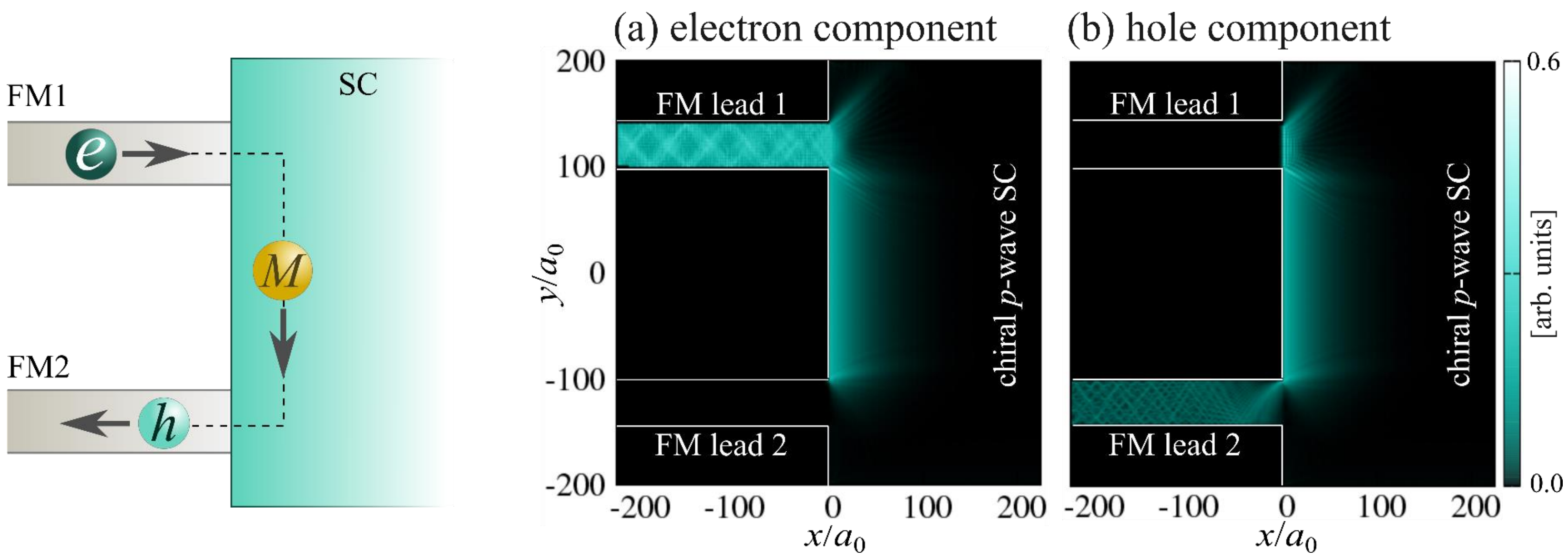

Long-ranged nonlocal transport is indeed mediated by the **CMESs**.

Conclusion (1)

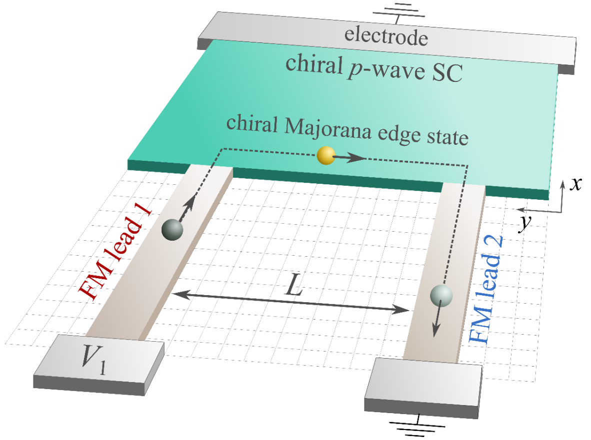

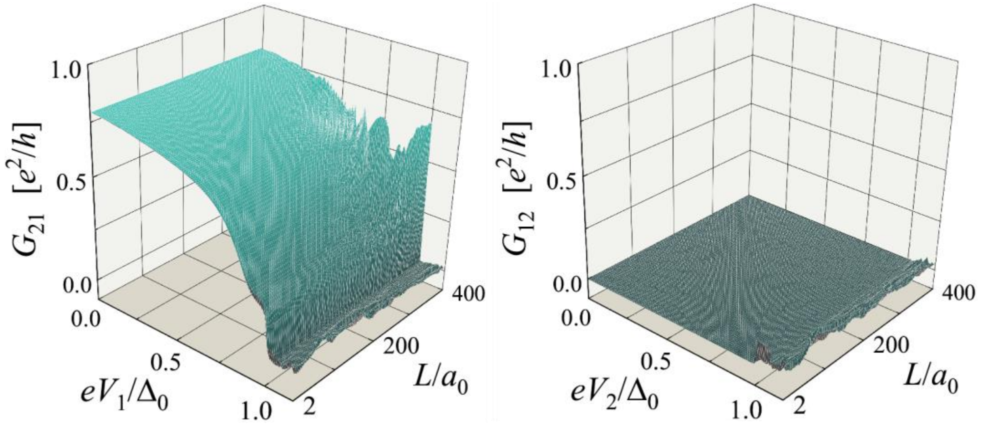

Distinct contrast between G_{21} and G_{12}
due to the **chiral motion** of the CMESs

Promising direction for obtaining
the **smoking-gun evidence** for the CMESs

Phys. Rev. Lett. **123**. 207002 (2019)

Sec. 2

Anomalous proximity effect of planar topological Josephson junctions

S. Ikegaya, S. Tamura, D. Manske, and Y. Tanaka

arXiv: 2007.12888

[PRB(R), in publication]

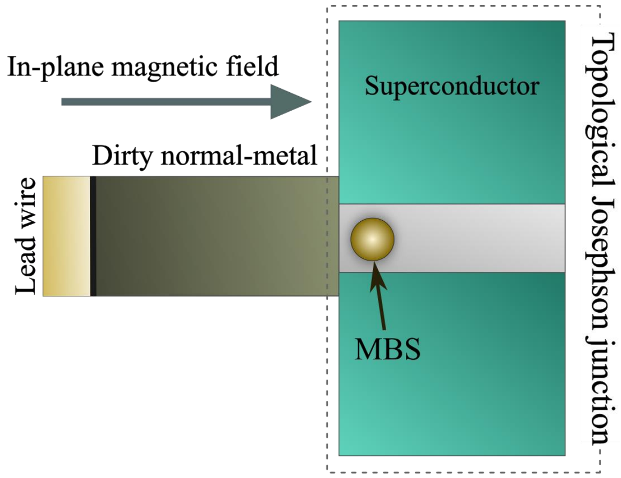

Anomalous proximity effect

- spin-singlet s-wave

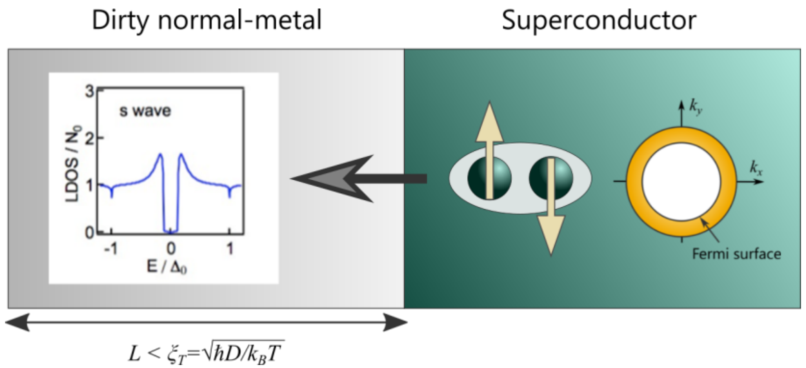

- gapped DOS
- reduction in resistance
- diamagnetism

Superconductivity-like

- spin-triplet p-wave

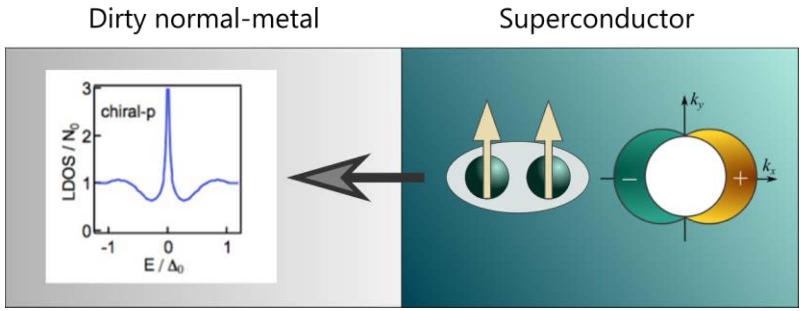

- zero-energy peak in DOS
- zero-bias conductance peak
- paramagnetism

Counter-intuitive!
Anomalous!

Y. Tanaka, *et al.*, PRB(2004)

Majorana bound states

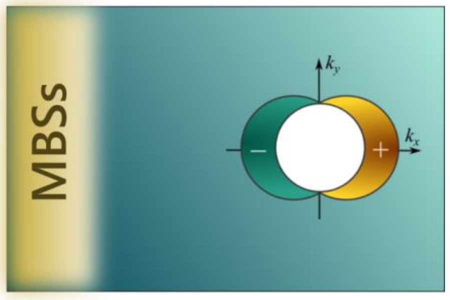

- **Majorana bound states (MBSs)**
  - particle = anti-particle ($\gamma = \gamma^\dagger$)
  - topologically protected

Majorana bound states

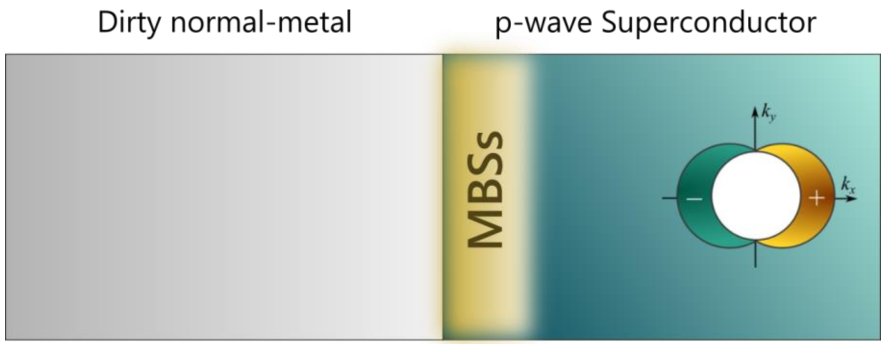

- **Majorana bound states (MBSs)**
  - particle = anti-particle ($\gamma = \gamma^\dagger$)
  - topologically protected

Majorana bound states

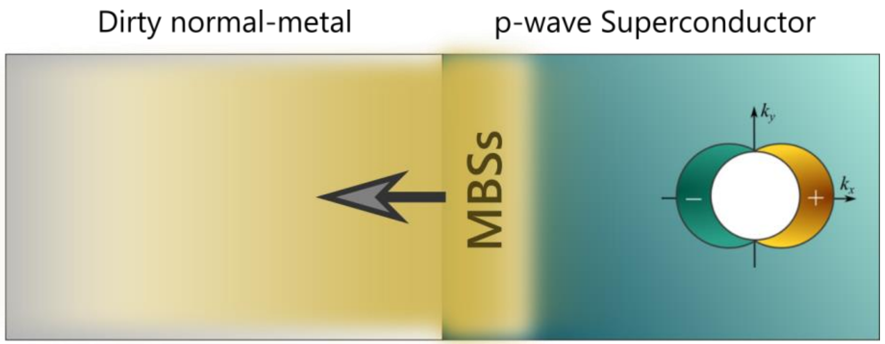

- Majorana bound states (MBSs)
  - particle = anti-particle ($\gamma = \gamma^\dagger$)
  - topologically protected

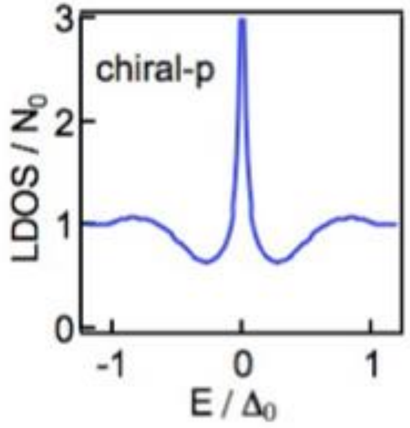

- **Penetration of MBSs**
  - Zero-energy peak in DOS Y. Tanaka, *et al*., PRB(2004)
  - Resonant states at zero-energy SI, *et al*., PRB(2015)

Odd-frequency Cooper pairs

p-wave superconductor

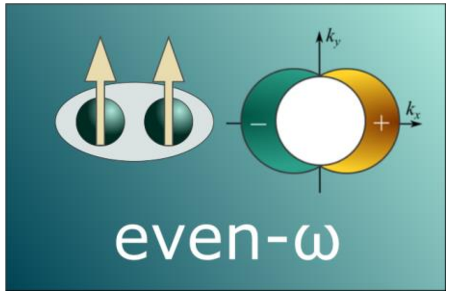

- **Pairing symmetry**: $F_{\sigma\sigma'}(r, r', \omega) = -F_{\sigma'\sigma}(r', r, -\omega)$

spin × parity × frequency $= \mathbf{-1}$

Y. Tanaka, *et al.*, PRL(2007), Y. Asano, *et al.*, PRL(2011), S.-I. Suzuki, *et al.*, PRL(2014)

Odd-frequency Cooper pairs

p-wave superconductor

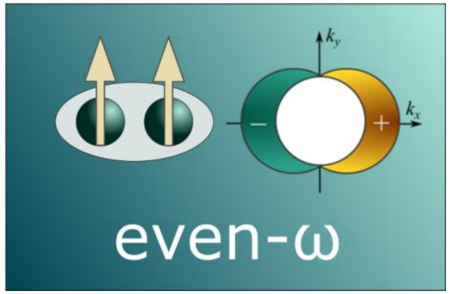

- **Pairing symmetry**: $F_{\sigma\sigma'}(r, r', \omega) = -F_{\sigma'\sigma}(r', r, -\omega)$

	spin	× parity	× frequency	$= -\mathbf{1}$
SC	triplet (even)	p-wave (odd)	even-ω	

Y. Tanaka, *et al.*, PRL(2007), Y. Asano, *et al.*, PRL(2011), S.-I. Suzuki, *et al.*, PRL(2014)

Odd-frequency Cooper pairs

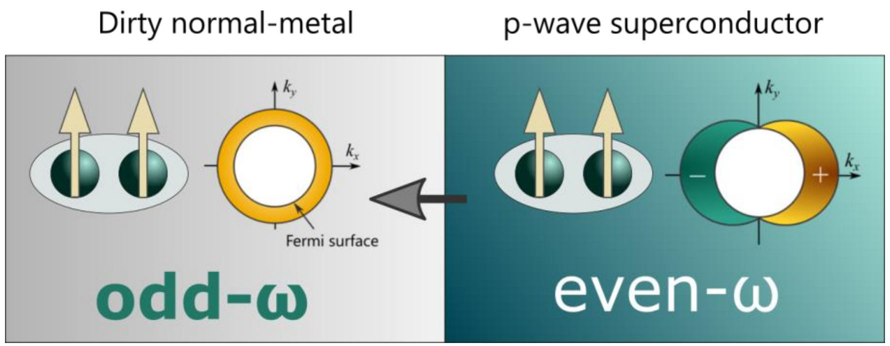

- **Pairing symmetry**: $F_{\sigma\sigma'}(r, r', \omega) = -F_{\sigma'\sigma}(r', r, -\omega)$

	spin ×	parity ×	frequency = -1
SC	triplet (even)	p-wave (odd)	even-ω
dirty N	triplet	s-wave	odd-ω

➡ **Paramagnetic response**

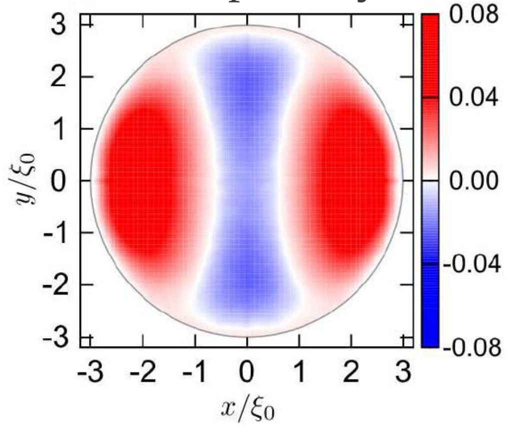

Y. Tanaka, *et al.*, PRL(2007), Y. Asano, *et al.*, PRL(2011), S.-I. Suzuki, *et al.*, PRB(2014)

Important problem

Anomalous proximity effect

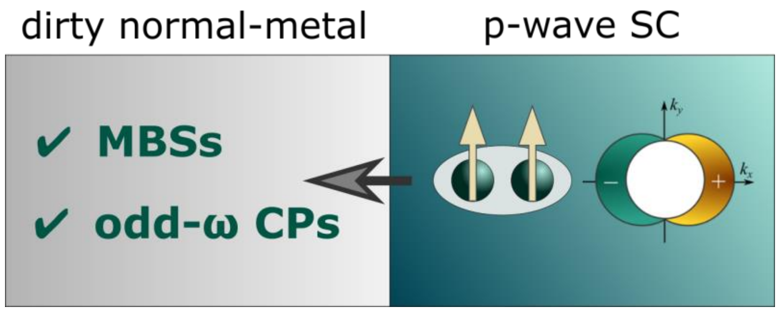

- zero-energy peak in DOS
- zero-bias conductance peak

→ **Majorana bound states**

- paramagnetism

→ **Odd-frequency Cooper pairs**

Important problem

Anomalous proximity effect

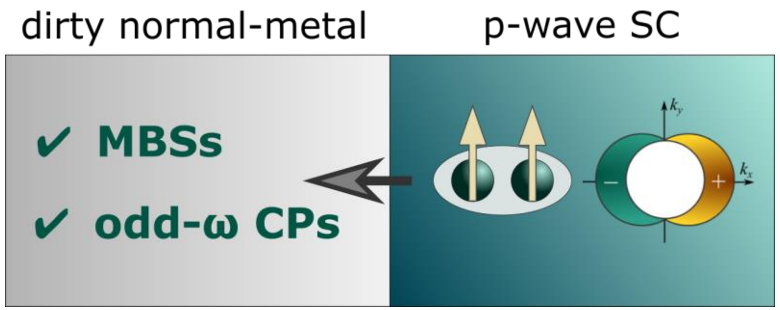

- zero-energy peak in DOS
- zero-bias conductance peak

→ Majorana bound states

- paramagnetism

→ Odd-frequency Cooper pairs

No experimental evidences so far

Crucial lack of suitable superconducting systems

Planar topological Josephson junction

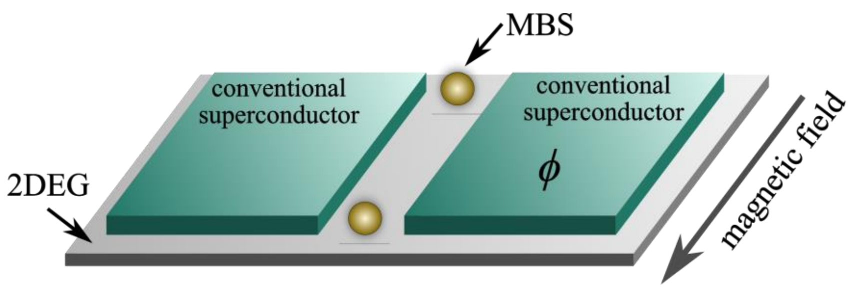

F. Pientka, *et al.*, PRX (2017)

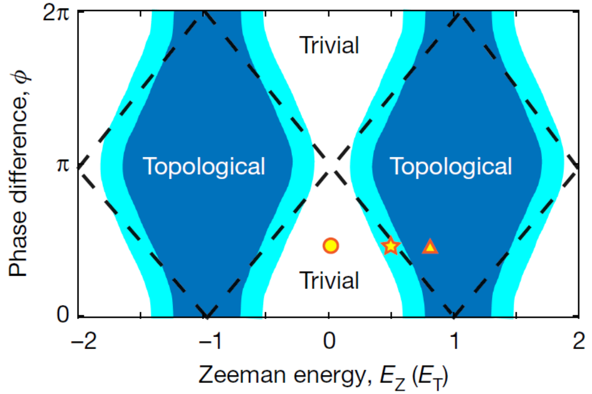

MBSs in a superconductor/thin film semiconductor hybrid

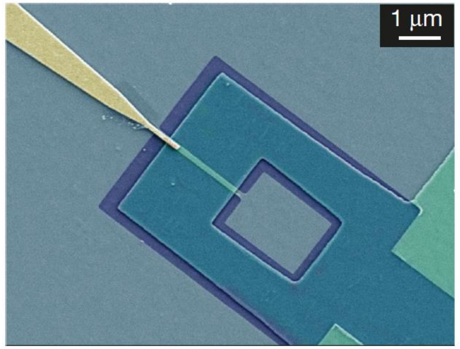

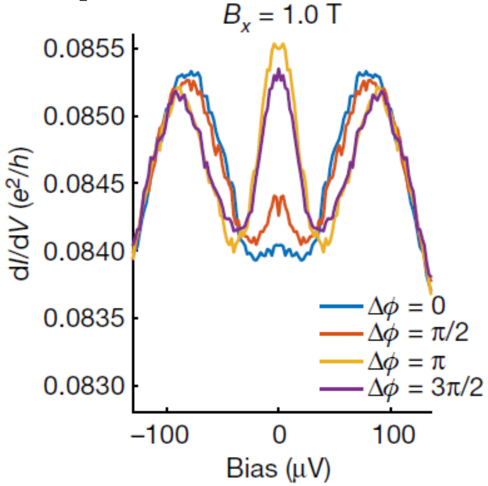

Fabrication techniques are well established!

Already realized in experiments!

H. Ren, *et al.*, Nature (2019)

A. Fornieri, *et al.*, Nature (2019)

W. Mayer, *et al.*, arXiv: 1906.01179(2019)

What we additionally need is a dirty normal-metal.

Objective (2)

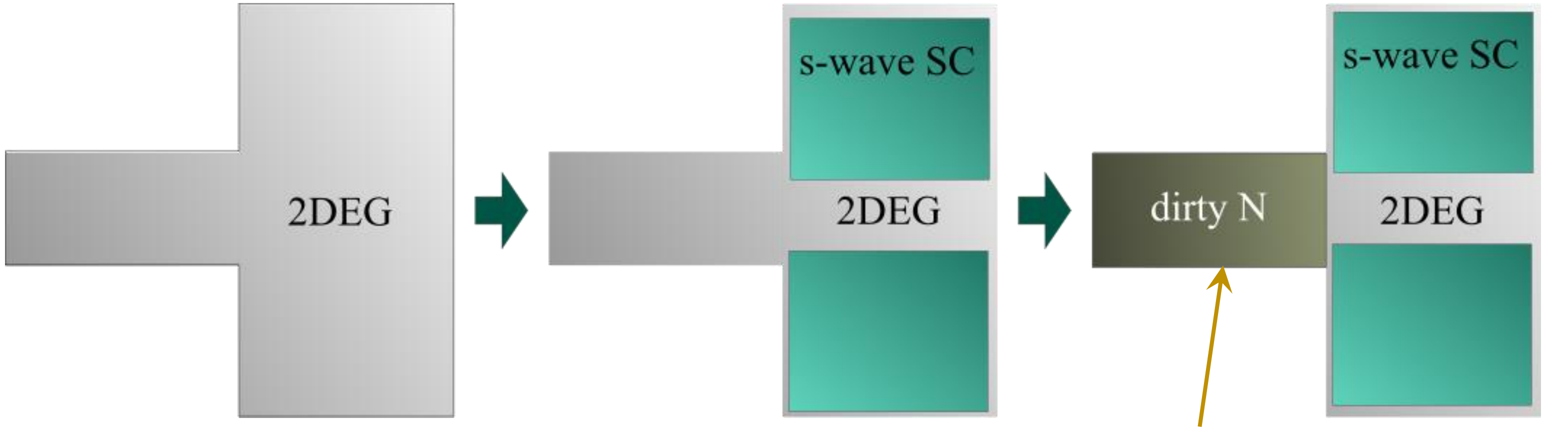

(e.g.) Focused ion beam techniques

Objective (2)

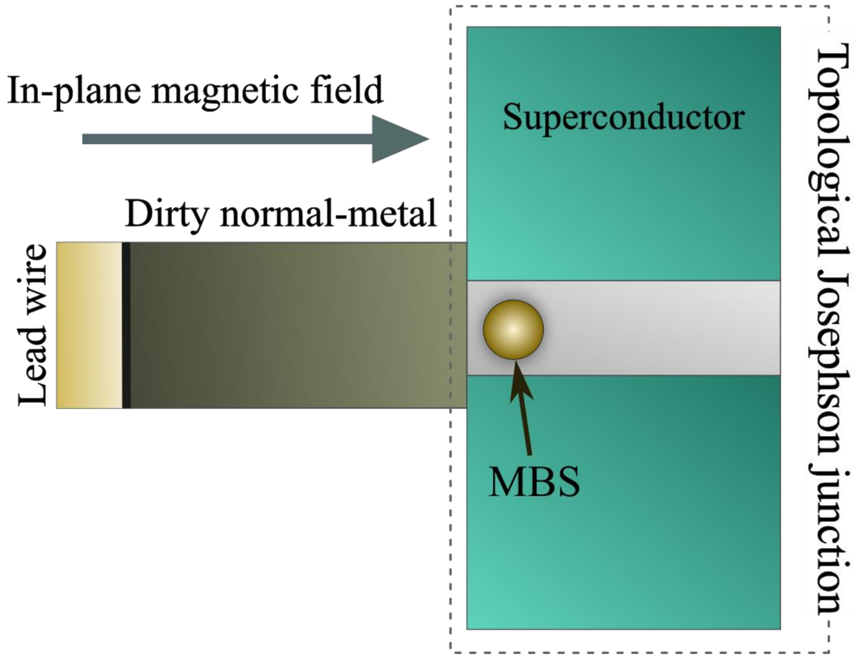

We study the anomalous proximity effect of topological Josephson junctions.

Model and Formulation

Topological Josephson junction

$$H = H_N + H_\Delta$$

$$\begin{aligned} H_N =& -t \sum_{\langle \boldsymbol{r},\boldsymbol{r}'\rangle,\sigma} \left[c^\dagger_{\boldsymbol{r},\sigma} c_{\boldsymbol{r}',\sigma} + \text{h.c.}\right] - \mu \sum_{\boldsymbol{r},\sigma} c^\dagger_{\boldsymbol{r},\sigma} c_{\boldsymbol{r},\sigma} \\ &+ \frac{i\lambda}{2} \sum_{\boldsymbol{r},\sigma,\sigma'} (\sigma_y)_{\sigma,\sigma'} \left[c^\dagger_{\boldsymbol{r}+\boldsymbol{x},\sigma} c_{\boldsymbol{r},\sigma'} - c^\dagger_{\boldsymbol{r},\sigma} c_{\boldsymbol{r}+\boldsymbol{x},\sigma'}\right] \\ &- \frac{i\lambda}{2} \sum_{\boldsymbol{r},\sigma,\sigma'} (\sigma_x)_{\sigma,\sigma'} \left[c^\dagger_{\boldsymbol{r}+\boldsymbol{y},\sigma} c_{\boldsymbol{r},\sigma'} - c^\dagger_{\boldsymbol{r},\sigma} c_{\boldsymbol{r}+\boldsymbol{y},\sigma'}\right] \\ &+ V_Z \sum_{\boldsymbol{r},\sigma,\sigma'} (\sigma_x)_{\sigma,\sigma'} c^\dagger_{\boldsymbol{r},\sigma} c_{\boldsymbol{r},\sigma'}, \end{aligned} \tag{1}$$

$$\begin{aligned} H_\Delta =& \sum_j \sum_{m=1}^{W_S} \left[\Delta e^{i\varphi/2} c^\dagger_{\boldsymbol{r},\uparrow} c^\dagger_{\boldsymbol{r},\downarrow} + \text{h.c.}\right] \\ &+ \sum_j \sum_{m=1+W_S}^{W_N+W_S} \left[\Delta e^{-i\varphi/2} c^\dagger_{\boldsymbol{r},\uparrow} c^\dagger_{\boldsymbol{r},\downarrow} + \text{h.c.}\right], \end{aligned} \tag{2}$$

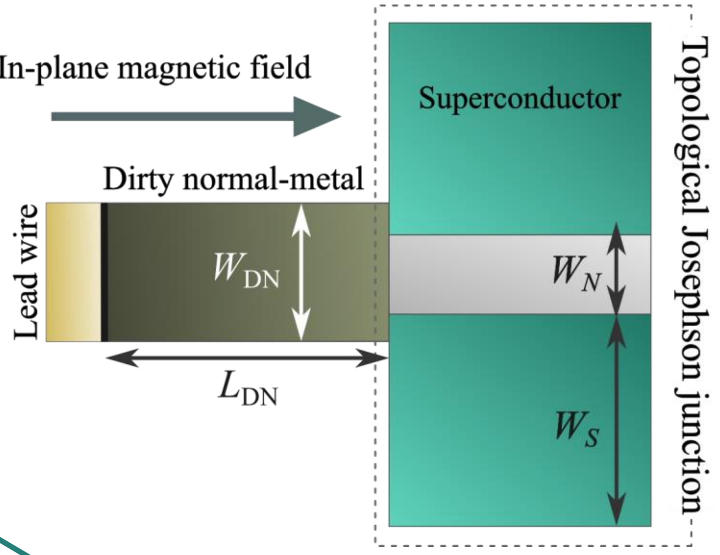

Rashba spin-orbit coupling

Zeeman potential

s-wave pair potential

Model and Formulation

Dirty normal-metal

$$H_{\mathrm{DN}} = H_N + H_{\mathrm{DP}}$$

$$\begin{aligned} H_N =& -t \sum_{\langle \boldsymbol{r},\boldsymbol{r}'\rangle,\sigma} \left[c^\dagger_{\boldsymbol{r},\sigma} c_{\boldsymbol{r}',\sigma} + \mathrm{h.c.}\right] - \mu \sum_{\boldsymbol{r},\sigma} c^\dagger_{\boldsymbol{r},\sigma} c_{\boldsymbol{r},\sigma} \\ &+ \frac{i\lambda}{2} \sum_{\boldsymbol{r},\sigma,\sigma'} (\sigma_y)_{\sigma,\sigma'} \left[c^\dagger_{\boldsymbol{r}+\boldsymbol{x},\sigma} c_{\boldsymbol{r},\sigma'} - c^\dagger_{\boldsymbol{r},\sigma} c_{\boldsymbol{r}+\boldsymbol{x},\sigma'}\right] \\ &- \frac{i\lambda}{2} \sum_{\boldsymbol{r},\sigma,\sigma'} (\sigma_x)_{\sigma,\sigma'} \left[c^\dagger_{\boldsymbol{r}+\boldsymbol{y},\sigma} c_{\boldsymbol{r},\sigma'} - c^\dagger_{\boldsymbol{r},\sigma} c_{\boldsymbol{r}+\boldsymbol{y},\sigma'}\right] \\ &+ V_Z \sum_{\boldsymbol{r},\sigma,\sigma'} (\sigma_x)_{\sigma,\sigma'} c^\dagger_{\boldsymbol{r},\sigma} c_{\boldsymbol{r},\sigma'}, \end{aligned} \tag{1}$$

$$H_{\mathrm{DP}} = \sum_{\boldsymbol{r},\sigma} v(\boldsymbol{r}) c^\dagger_{\boldsymbol{r},\sigma} c_{\boldsymbol{r},\sigma}, \tag{3}$$

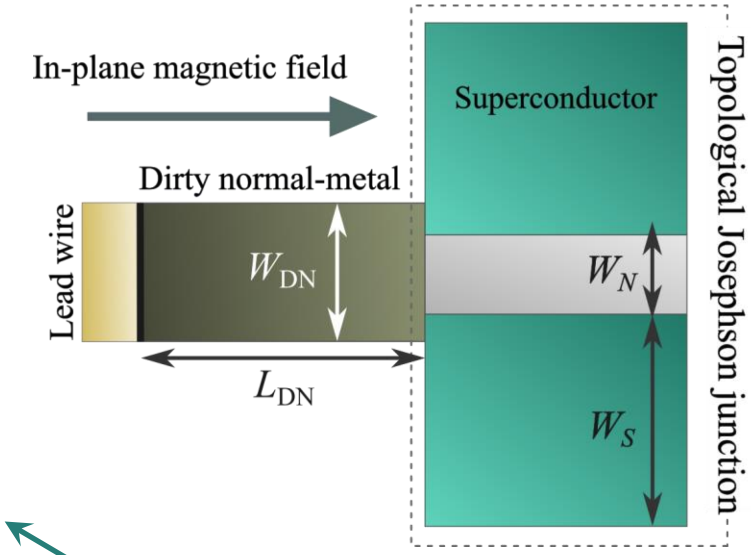

Rashba spin-orbit coupling

Zeeman potential

Random onsite potential

Model and Formulation

Lead wire

$$H' = -t' \sum_{\langle \boldsymbol{r},\boldsymbol{r}'\rangle,\sigma} [c^\dagger_{\boldsymbol{r},\sigma} c_{\boldsymbol{r}',\sigma} + \mathrm{h.c.}] - \mu' \sum_{\boldsymbol{r},\sigma} c^\dagger_{\boldsymbol{r},\sigma} c_{\boldsymbol{r},\sigma}$$
$$+ V'_Z \sum_{\boldsymbol{r},\sigma,\sigma'} (\sigma_x)_{\sigma,\sigma'} c^\dagger_{\boldsymbol{r},\sigma} c_{\boldsymbol{r},\sigma'}, \qquad (4)$$

Zeeman potential

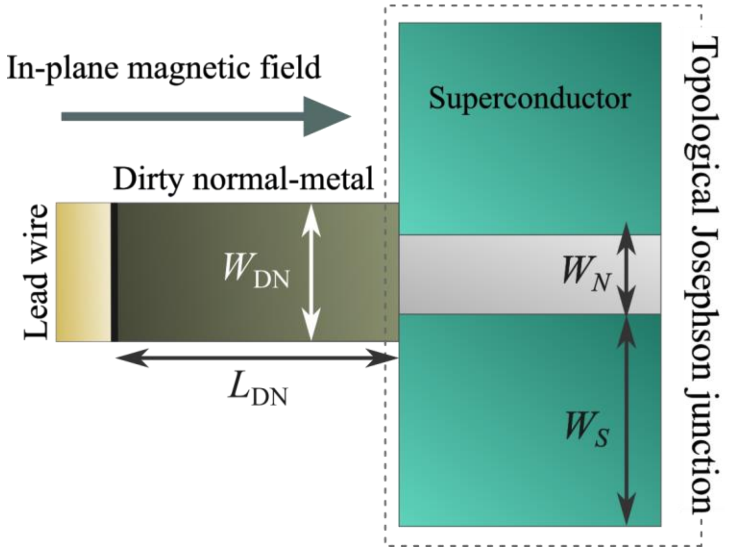

- Bad transparency at the lead-wire/dirty normal-metal interface.

Differential conductance

Blonder-Tinkham-Klapwijk formula

$$G_{NS}(eV) = \frac{e^2}{h} \sum_{\alpha\beta} \left(1 + \left|r^{he}_{\alpha\beta}(E)\right|^2 - \left|r^{ee}_{\alpha\beta}(E)\right|^2\right)_{E\,=\,eV}$$

Topological phase diagram

- Topological phase diagram

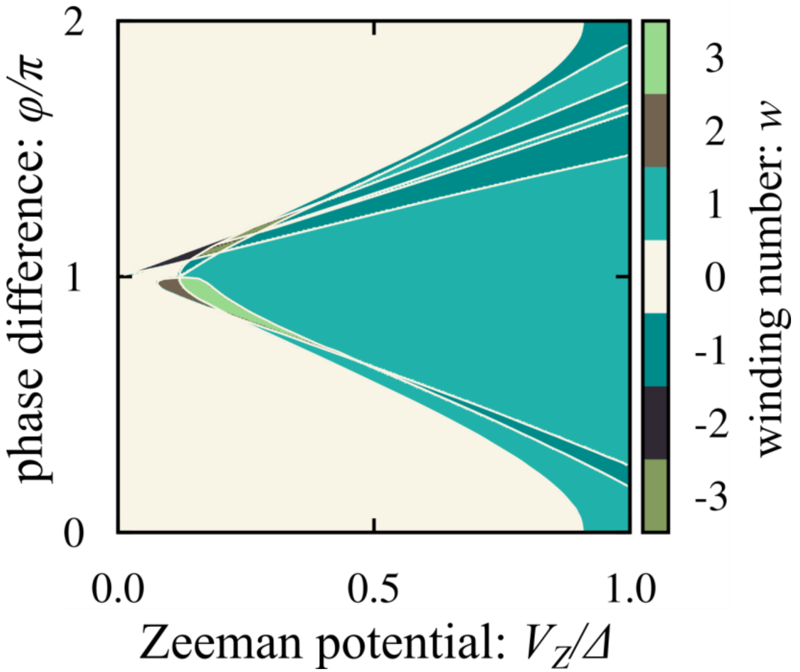

$$\mathbb{Z}_2 = (-1)^w$$

$$w = \frac{1}{4\pi i}\int dk_x \mathrm{Tr}\left[\check{S}\check{H}^{-1}(k_x)\partial_{k_x}\check{H}(k_x)\right]$$

$$\check{S}\,\check{H}(k_x)\,\check{S} = -\check{H}(k_x)$$

F. Pientka, *et al.*, PRX (2017)

Odd winding number: *w* ➡ **Robust MBSs**

Differential conductance

Zero-bias conductance(ZBC)

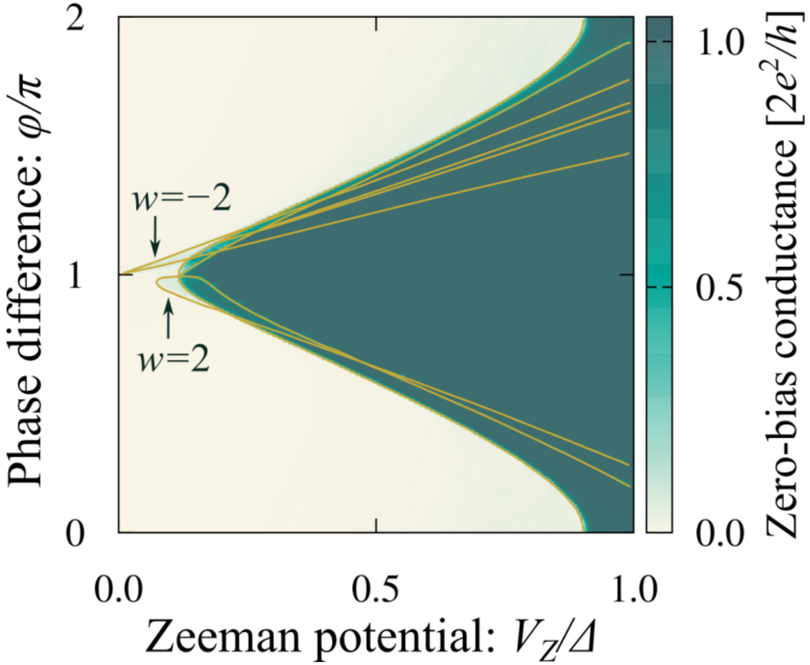

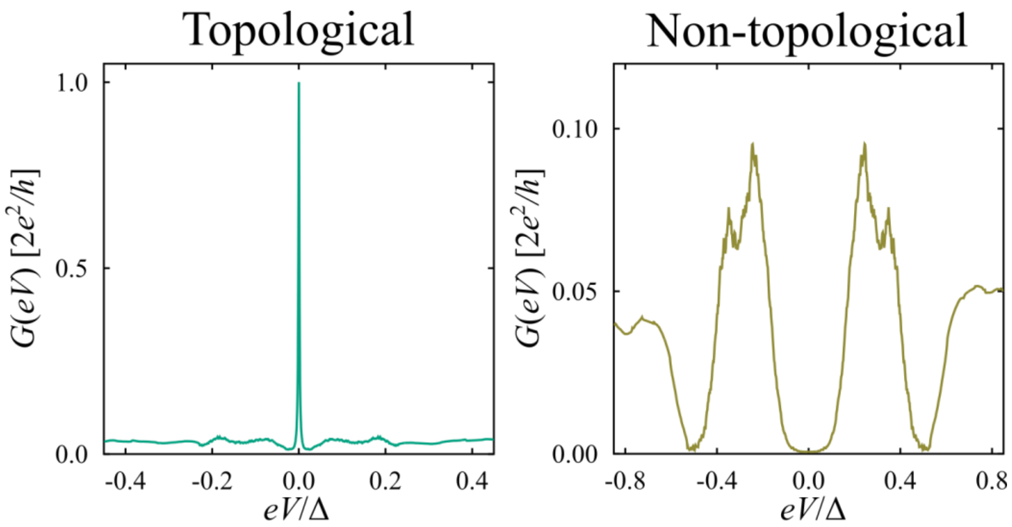

- **ZBC quantization only in the topological phase**
  (irrespective of disordered potentials)
- **Drastic change in the conductance spectrum**

Penetration of MBSs

LDOS in the DN segment

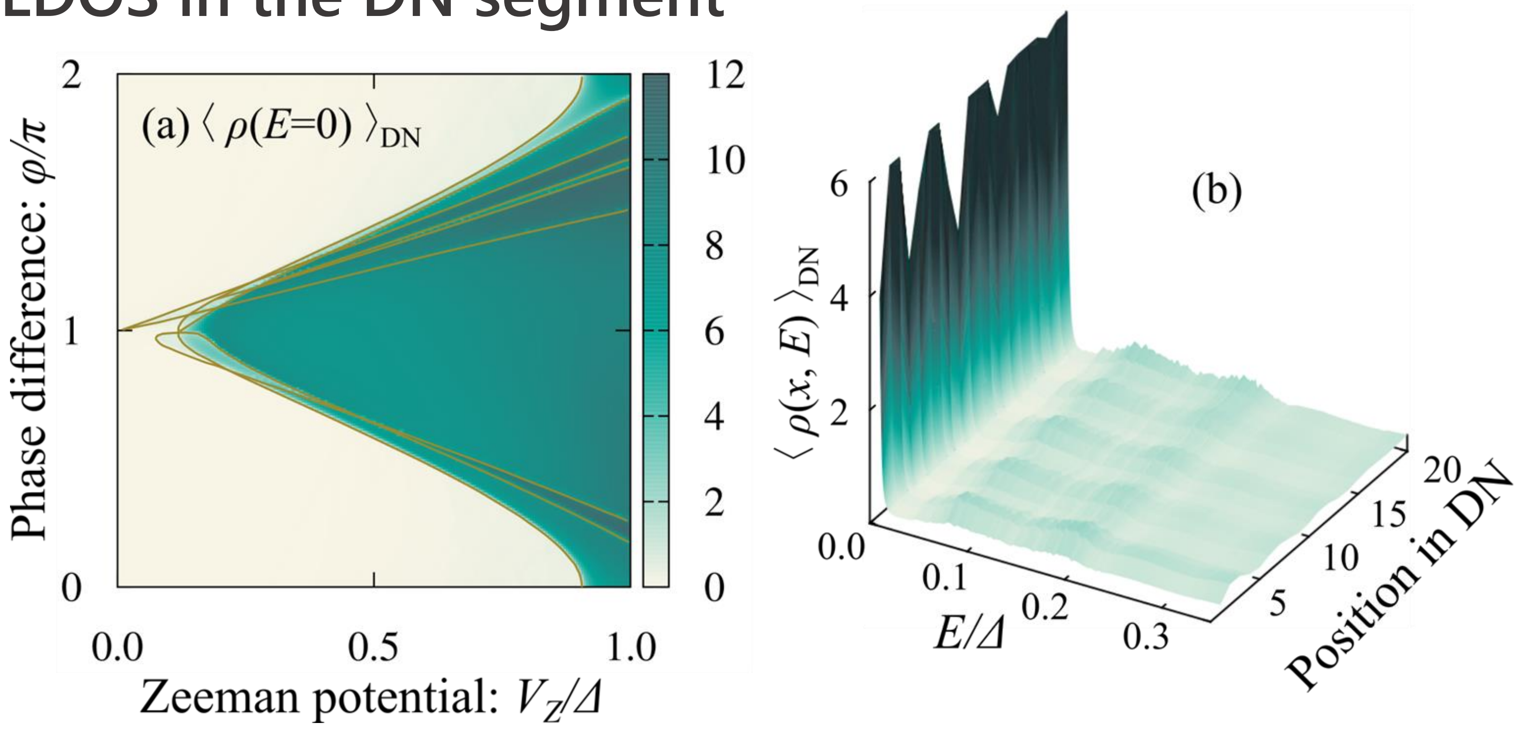

Zero-energy peak only in the topological phase

Penetration of the Majorana bound states

Penetration of odd-ω Cooper pairs

Odd-ω pair amplitude

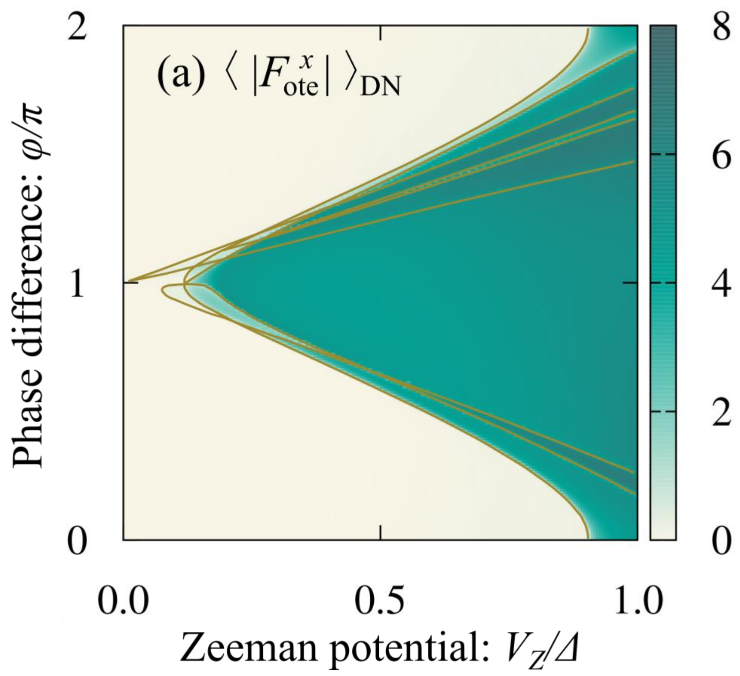

$$F_{\mathrm{ote}}(r,r,\omega) = \frac{F(r,r,\omega) - F(r,r,-\omega)}{2}$$

$(\omega \ll \Delta)$

Significant amplitude only in the topological phase

⬇

Penetration of the odd-ω Cooper pairs

Conclusion (2)

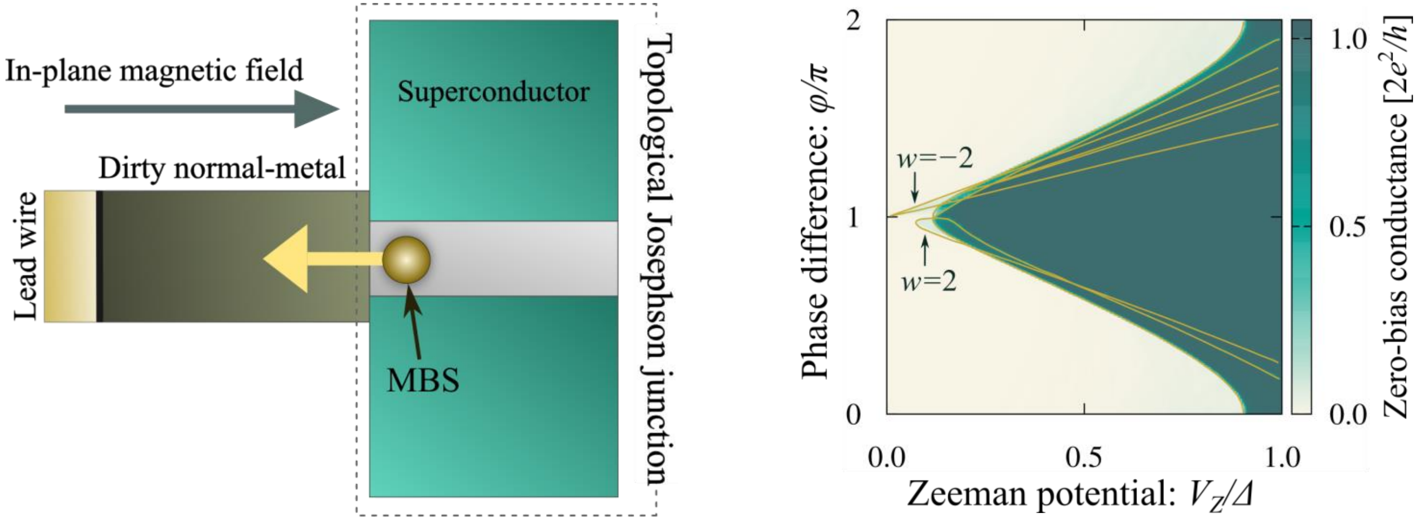

Anomalous proximity effect in
a **planar topological Josephson junction**

Promising for achieving the **first experimental observation**

arXiv: 2007.12888
[PRB(R), in publication]

Sec. 4

Summary

Summary

Proving profound natures of topological edge states!

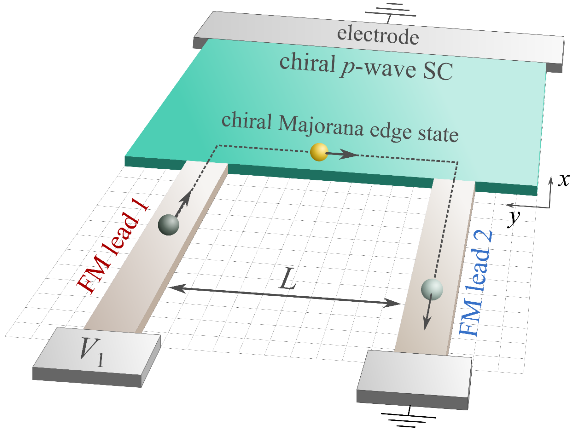

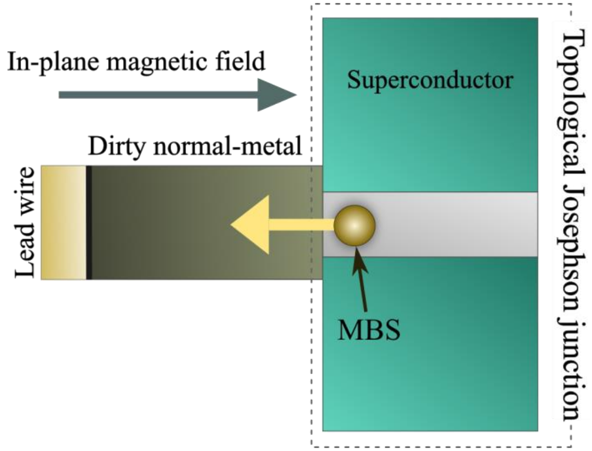

- Anomalous nonlocal conductance as a fingerprint of chiral Majorana edge states   Phys. Rev. Lett. 123, 207002 (2019)

➡ **Applicable to UTe_2**

- Anomalous proximity effect of planar topological Josephson junctions

➡ **Promising for the first experimental observation**

arXiv: 2007.12888
[PRB(R), in publication]

Thank you !